

1 **Development of CpG-adjuvanted stable prefusion SARS-CoV-2 spike**  
2 **antigen as a subunit vaccine against COVID-19**

3

4 Tsun-Yung Kuo<sup>1, 2</sup>, Meei-Yun Lin<sup>1</sup>, Robert L Coffman<sup>3</sup>, John D Campbell<sup>3</sup>, Paula Traquina<sup>3</sup>, Yi-Jiun  
5 Lin<sup>1</sup>, Luke Tzu-Chi Liu<sup>1</sup>, Jinyi Cheng<sup>1</sup>, Yu-Chi Wu<sup>1</sup>, Chung-Chin Wu<sup>1</sup>, Wei-Hsuan Tang<sup>1</sup>, Chung-Guei  
6 Huang<sup>4,5</sup>, Kuo-Chien Tsao<sup>4,5</sup>, Shin-Ru Shih<sup>4,5</sup>, Charles Chen<sup>1,6\*</sup>

7

8 <sup>1</sup>Medigen Vaccine Biologics Corporation, Taipei City, Taiwan

9 <sup>2</sup>Department of Biotechnology and Animal Science, National Ilan University, Yilan County, Taiwan

10 <sup>3</sup>Dynavax Technologies, Emeryville, CA 94608, USA

11 <sup>4</sup>Department of Laboratory Medicine, Linkou Chang Gung Memorial Hospital, Taoyuan City, Taiwan

12 <sup>5</sup>Research Center for Emerging Viral Infections, College of Medicine, Chang Gung University,

13 Taoyuan City, Taiwan

14 <sup>6</sup>Adjunct Professor of College of Science and Technology, Temple University, Philadelphia, PA

15 19122, USA

16 \*Corresponding author: charles@medigenvac.com

17 **Abstract**

18

19 The COVID-19 pandemic caused by the novel coronavirus SARS-CoV-2 is a worldwide health emergency.  
20 The immense damage done to public health and economies has prompted a global race for cures and vaccines.  
21 In developing a COVID-19 vaccine, we applied technology previously used for MERS-CoV to produce a  
22 prefusion-stabilized SARS-CoV-2 spike protein by adding two proline substitutions at the top of the central  
23 helix (S-2P). To enhance immunogenicity and mitigate the potential vaccine-induced immunopathology, CpG  
24 1018, a Th1-biasing synthetic toll-like receptor 9 (TLR9) agonist was selected as an adjuvant candidate. S-2P  
25 was combined with various adjuvants, including CpG 1018, and administered to mice to test its effectiveness in  
26 eliciting anti-SARS-CoV-2 neutralizing antibodies. S-2P in combination with CpG 1018 and aluminum  
27 hydroxide (alum) was found to be the most potent immunogen and induced high titer of spike-specific antibodies  
28 in sera of immunized mice. The neutralizing abilities in pseudotyped lentivirus reporter or live wild-type SARS-  
29 CoV-2 were measured with reciprocal inhibiting dilution (ID<sub>50</sub>) titers of 5120 and 2560, respectively. In addition,  
30 the antibodies elicited were able to cross-neutralize pseudovirus containing the spike protein of the D614G  
31 variant, indicating the potential for broad spectrum protection. A marked Th-1 dominant response was noted  
32 from cytokines secreted by splenocytes of mice immunized with CpG 1018 and alum. No vaccine-related  
33 serious adverse effects were found in the dose-ranging study in rats administered single- or two-dose regimens  
34 with up to 50 µg of S-2P combined with CpG 1018 alone or CpG 1018 with alum. These data support continued  
35 development of CHO-derived S-2P formulated with CpG 1018/alum as a candidate vaccine to prevent COVID-  
36 19 disease.

37 **Introduction**

38

39 COVID-19 was first identified as a cause of severe pneumonia cases in December 2019 in association with  
40 a seafood market in Wuhan, China [1]. The viral agent was identified as a novel SARS-like coronavirus (SARS-  
41 CoV-2) most closely related to bat coronavirus [1]. In the six months since its first appearance, SARS-CoV-2  
42 has become the largest pandemic since the 1918 influenza with nearly 20 million infected and over 700,000  
43 deaths worldwide as of August 2020 [2, 3]. The rapid spread and huge socioeconomic impact of this pandemic  
44 require the urgent development of effective countermeasures, including vaccines. In response, pharmaceuticals,  
45 academia, and institutions are developing vaccines and drugs at an unprecedented pace with governments and  
46 foundations pledging hundreds of millions of dollars for COVID-19 research [4].

47

48 In addition to basic public health control measures such as social distancing, contact tracing and quarantine,  
49 a safe and effective vaccine is the only weapon that can potentially offer lasting protection against COVID-19  
50 and stop the current pandemic. According to the WHO, 26 vaccine candidates using various platforms have  
51 entered clinical trials as of July 31, 2020 [5]. These candidate vaccines have all been developed in compliance  
52 with WHO guidelines that define desired characteristics such as dose regimen, target population, safety,  
53 measures of efficacy, and requirements for product stability and storage [6].

54

55 Coronaviruses are among the largest known enveloped RNA viruses and cause respiratory illnesses in  
56 humans ranging from the common cold to SARS, MERS, as well as the current COVID-19 pandemic [7].  
57 Similar to SARS-CoV, the spike (S) protein of SARS-CoV-2 is the receptor for attachment and cell entry via  
58 the cellular receptor hACE2 [1]. Researchers are also adapting antigen design strategies used for SARS-CoV  
59 and MERS-CoV spike proteins to develop a candidate vaccine for SARS-CoV-2. A stabilized prefusion form  
60 of the MERS spike protein was achieved in 2017 by transferring two proline substitutions between heptad repeat  
61 1 and the central helix analogous to those defined in the HKU1 spike protein. These mutations together with a  
62 C-terminus foldon trimerization domain stabilized the spike ectodomain in its prefusion state resulting in a more

63 potent immunogen with dose-sparing properties compared to protein made with the original wild-type sequence  
64 [8]. The analogous mutations in the SARS-CoV-2 spike resulted in a homogeneous population of proteins  
65 allowing the atomic-level structure to be solved by cryo-electron microscopy [9].

66

67 Subunit vaccines such as the spike protein are often poorly immunogenic by themselves and therefore  
68 typically require adjuvants to enhance their ability to produce an immune response [10]. Adjuvants can be  
69 classified based on their properties into several categories, including aluminum salt-based (aluminum hydroxide  
70 and aluminum phosphate), oil emulsion-based such MF59 and AS03, and toll-like receptor (TLR) agonists,  
71 including CpG 1018 and monophosphoryl lipid A (AS04) [11]. A previous study employing four different  
72 candidate vaccines against SARS-CoV, all of them with and without alum adjuvants successfully elicited  
73 neutralizing antibodies and conferred protection against infection; however, tissue damage due to  
74 immunopathology was also observed from infiltrating lymphocytes [12]. Historical evidence from animal  
75 models suggests, vaccine-primed Th2 and Th17 responses may be associated with immunopathology referred  
76 to as vaccine-associated enhanced respiratory disease (VAERD) [13]; therefore, extra caution must be taken in  
77 the choice of adjuvants. Synthetic oligodeoxynucleotides with CpG motifs (CpG ODN) are agonists for TLR9  
78 and mimic the activity of naturally occurring CpG motifs found in bacterial DNA. CpG ODN are potent vaccine  
79 adjuvants generating Th1-biased responses, thus making them a good choice to mitigate potential Th2 and Th17  
80 induced immunopathology [11]. CpG 1018, a 22-mer CpG ODN containing sequence with a modified  
81 phosphorothioate backbone [14], is the adjuvant used in the licensed hepatitis B vaccine HEPLISAV-B®, and  
82 is the only TLR9 agonist used in an approved vaccine.

83

84 In this study, we present data from preclinical studies aimed at developing a COVID-19 candidate subunit  
85 vaccine using CHO cell-expressed SARS-CoV-2 S-2P antigen combined with various adjuvants. We have  
86 shown that S-2P, when mixed with CpG 1018 and aluminum hydroxide adjuvants, was most effective in  
87 inducing antibodies that neutralized pseudovirus and wild-type live virus while minimizing Th2-biased  
88 responses with no vaccine-related adverse effects.

89 **Materials and Methods**

90

91 **Production of S-2P protein ectodomains from Expi293 and ExpiCHO-S cells**

92        The plasmid expressing SARS-CoV-2 (strain Wuhan-Hu-1 GenBank: MN908947) S protein ectodomain  
93        was obtained from Dr. Barney S. Graham (Vaccine Research Center, National Institute of Allergy and Infectious  
94        Diseases, USA) and contains a mammalian-codon-optimized gene encoding SARS-CoV-2 S residues 1–1208  
95        with a C-terminal T4 fibritin trimerization domain, an HRV3C cleavage site, an 8×His-tag and a Twin-Strep-  
96        tag [9]. The S-2P form was created by mutation of the S1/S2 furin-recognition site 682-RRAR-685 to GSAS to  
97        produce a single-chain S0 protein, and the 986-KV-987 was mutated to PP [9].

98        Expi293 and ExpiCHO-S cells (ThermoFisher) were transfected with the plasmid expressing S-2P protein  
99        ectodomains by ExpiFectamine 293 transfection kit and ExpiFectamine CHO transfection kit (ThermoFisher),  
100        respectively. The secreted S-2P protein was purified by affinity chromatography. Purification tags were  
101        removed by HRV3C protease digestion and the S-2P protein was further purified. The purified S-2P proteins  
102        produced from Expi293 and ExpiCHO-S cells were quantified by BCA assay (ThermoFisher), flash frozen in  
103        liquid nitrogen and then stored at -80 °C. The ExpiCHO-expressed S-2P were sent to the Electronic Microscopy  
104        Laboratory at the Advanced Technology Research Facility (National Cancer Institute) for cryo-EM  
105        confirmation.

106

107 **Pseudovirus production and titration**

108        To produce SARS-CoV-2 pseudoviruses, a plasmid expressing full-length wild-type Wuhan-Hu-1 strain  
109        SARS-CoV-2 spike protein was cotransfected into HEK293T cells with packaging and reporter plasmids  
110        pCMVΔ8.91 and pLAS2w.FLuc.Ppuro (RNAi Core, Academia Sinica), using TransIT-LT1 transfection reagent  
111        (Mirus Bio). Site-directed mutagenesis was used to generate the D614G variant by changing nucleotide at  
112        position 23403 (Wuhan-Hu-1 reference strain) from A to G. Mock pseudoviruses were produced by omitting  
113        the p2019-nCoV spike (WT). Seventy-two hours post-transfection, supernatants were collected, filtered, and  
114        frozen at -80 °C. The transduction unit (TU) of SARS-CoV-2 pseudotyped lentivirus was estimated by using

115 cell viability assay in response to the limited dilution of lentivirus. In brief, HEK-293T cells stably expressing  
116 human ACE2 gene were plated on 96-well plate one day before lentivirus transduction. For the titering of  
117 pseudovirus, different amounts of pseudovirus were added into the culture medium containing polybrene. Spin  
118 infection was carried out at 1,100 xg in 96-well plate for 30 minutes at 37°C. After incubating cells at 37°C for  
119 16 hr, the culture medium containing virus and polybrene were removed and replaced with fresh complete  
120 DMEM containing 2.5 µg/ml puromycin. After treating with puromycin for 48 hrs, the culture media was  
121 removed and cell viability was detected by using 10% AlarmaBlue reagents according to manufacturer's  
122 instruction. The survival rate of uninfected cells (without puromycin treatment) was set as 100%. The virus titer  
123 (transduction units) was determined by plotting the survival cells versus diluted viral dose.

124

125 **Pseudovirus-based neutralization assay**

126 HEK293-hAce2 cells ( $2 \times 10^4$  cells/well) were seeded in 96-well white isoplates and incubated for overnight.  
127 Sera were heated at 56°C for 30 min to inactivate complement and diluted in MEM supplemented with 2 %  
128 FBS at an initial dilution factor of 20, and then 2-fold serial dilutions were carried out (for a total of 8 dilution  
129 steps to a final dilution of 1:5120). The diluted sera were mixed with an equal volume of pseudovirus (1,000  
130 TU) and incubated at 37 °C for 1 hr before adding to the plates with cells. After the 1-hr incubation, the culture  
131 medium was replaced with 50 µL of fresh medium. On the following day, the culture medium was replaced  
132 with 100 µL of fresh medium. Cells were lysed at 72 hours post infections and relative luciferase units (RLU)  
133 was measured. The luciferase activity was detected by Tecan i-control (Infinite 500). The 50% and 90%  
134 inhibition dilution titers ( $ID_{50}$  and  $ID_{90}$ ) were calculated considering uninfected cells as 100% neutralization and  
135 cells transduced with only virus as 0% neutralization. Reciprocal  $ID_{50}$  and  $ID_{90}$  geometric mean titers (GMT)  
136 were both determined as  $ID_{90}$  titers are useful when  $ID_{50}$  titer levels are consistently saturating at the upper limit  
137 of detection.

138

139 **Wild-type SARS-CoV-2 neutralization assay**

140        The neutralization assay with SARS-CoV-2 virus was conducted as previously reported [15]. Vero E6 cells  
141        ( $2.5 \times 10^4$  cells/well) were seeded in 96-well plates and incubated overnight. Sera were heated at 56°C for 30 min  
142        to inactivate complement and diluted in serum-free MEM at an initial dilution factor of 20, and then further 2-  
143        fold serial dilutions were performed for a total 11 dilution steps to a final dilution of 1:40960. The diluted sera  
144        were mixed with an equal volume of SARS-CoV-2 virus at 100 TCID<sub>50</sub>/50 μL (hCoV-19/Taiwan/CGMH-CGU-  
145        01/2020, GenBank accession MT192759) and incubated at 37 °C for 2 hr. The sera-virus mixture was then  
146        added to 96-well plate with Vero E6 cells and incubated in MEM with 2% FBS at 37 °C for 5 days. After  
147        incubation, cells were fixed by adding 4% formalin to each of the wells for 10 min and stained with 0.1% crystal  
148        violet for visualization. Results were calculated with the Reed-Muench method for log 50% end point for ID<sub>50</sub>  
149        and log 90% end point for ID<sub>90</sub> titers.

150

## 151        **Animals**

152        BALB/cJ mice were obtained from the National Laboratory Animal Center, Academia Sinica, Taiwan and  
153        BioLASCO Taiwan Co. Ltd. Crl:CD® Sprague Dawley (SD) rats were obtained from BioLASCO Taiwan Co.  
154        Ltd. Animal studies were conducted in the Testing Facility for Biological Safety, TFBS Bioscience Inc., Taiwan.  
155        All animal work was reviewed and approved by the Institutional Animal Care and Use Committee (IACUC).  
156        The Testing Facility's IACUC animal study protocol approval numbers are TFBS2020-006 and TFBS2020-010.

157

## 158        **Immunization of mice**

159        For antigen formulation, 0.5 mL of SARS-CoV-2 S-2P protein was mixed with either an equal volume of  
160        Sigma Adjuvant System S6322 (Sigma), 600 μg/mL Adju-Phos aluminum phosphate (Brenntag), CpG 1018  
161        (200 μg/mL), aluminum hydroxide (1 mg/mL), PBS, or 0.25 mL CpG 1018 (400 μg/mL) plus 0.25 mL  
162        aluminum hydroxide (2 mg/mL). Female BALB/cJ mice aged 6–9 weeks were immunized twice at 3 weeks  
163        apart as previously described [8]. Total serum anti-S IgG levels were detected with direct ELISA using custom  
164        96-well plates coated with S-2P antigen.

165

166 **Cytokine assays**

167 Two weeks after the second injection, mice were euthanized and splenocytes were isolated and stimulated  
168 with S-2P protein (2  $\mu$ g/well) as previously described [16]. For detection of IFN- $\gamma$ , IL-2, IL-4, and IL-5, the  
169 culture supernatant from the 96-well microplates was harvested to analyze the levels of cytokines by ELISA  
170 using Mouse IFN- $\gamma$  Quantikine ELISA Kit, Mouse IL-2 Quantikine ELISA Kit, Mouse IL-4 Quantikine ELISA  
171 Kit, and Mouse IL-5 Quantikine ELISA Kit (R&D System). The OD450 values were read by Multiskan GO  
172 (ThermoFisher).

173

174 **Dose range finding study for single and repeat-dose intramuscular injection (IM) in Sprague Dawley  
175 (SD) Rats**

176 To investigate the safety of SARS-CoV-2 S-2P protein adjuvanted with CpG 1018 alone or combined with  
177 aluminum hydroxide, pilot toxicity studies were conducted for dose range finding. SD rats aged 6-8 weeks were  
178 immunized with 5  $\mu$ g, 25  $\mu$ g or 50  $\mu$ g of S-2P adjuvanted with either CpG 1018 alone or CpG 1018 combined  
179 with aluminum hydroxide. The test article or vehicle control was administered intramuscularly to each rat on  
180 Day 1 (for single-dose study) and Day 15 (for repeat-dose study). The observation period was 14 days (for  
181 single-dose study) and 28 days (for repeat-dose study). Parameters evaluated included clinical signs, local  
182 irritation examination, moribundity/mortality, body temperature, body weights, and food consumption during  
183 the in-life period. Blood samples were taken for hematology, including coagulation tests and serum chemistry.  
184 All animals were euthanized and necropsied for gross lesion examination, organ weights, and histopathology  
185 evaluation on injection sites and lungs.

186

187 **Statistical analysis**

188 For neutralization assays, geometric mean titers are represented by the heights of bars with 95% confidence  
189 intervals represented by the error bars. For cytokine and rat data, heights of bars or symbols represent means  
190 with SD represented by error bars.

191 Dotted lines represent lower and upper limits of detection. Mann-Whitney U-test included in the analysis  
192 package in Prism 6.01 (GraphPad) was used to compare between two experimental groups. \* =  $p < 0.05$ , \*\* =  
193  $p < 0.01$ , \*\*\* =  $p < 0.001$

194

## 195 **Results**

196

### 197 **Adjuvanted SARS-CoV-2 S-2P induced robust neutralizing antibodies**

198 Sera of BALB/cJ mice vaccinated with HEK293-expressed S-2P with or without adjuvants were assessed  
199 using pseudovirus neutralization assays for immunogenicity elicited by S-2P antigen. Reciprocal ID<sub>50</sub> and ID<sub>90</sub>  
200 geometric mean titers (GMT) were determined as ID<sub>90</sub> titer is useful when ID<sub>50</sub> titer levels are consistently  
201 saturating at the upper limit of detection. At 1  $\mu$ g of S-2P, the ID<sub>50</sub> titers of S-2P alone, with aluminum phosphate,  
202 and with Sigma Adjuvant were 259, 2,124, and 5,099, respectively; whereas the ID<sub>90</sub> titers of the above were  
203 41, 282, and 2007, respectively (Figure S1).

204 Additional immunogenicity studies were conducted to test the adjuvanted vaccine in different antigen  
205 dosages. Similar results were obtained as in the previous experiment (Figure S2). Likewise, both ID<sub>50</sub> and ID<sub>90</sub>  
206 titers induced by higher antigen dose was stronger than that induced by lower antigen dose. Taken together,  
207 these data again confirmed that SARS-CoV-2 S-2P combined with adjuvants induced effective neutralizing  
208 antibody, thus indicating early potential and preliminary evidence to pursue development of this candidate  
209 COVID-19 vaccine.

210

### 211 **Induction of potent neutralizing antibodies by CpG 1018 and aluminum hydroxide-adjuvanted S-2P**

212 Having established the ability of Expi293-expressed S-2P to induce neutralizing antibodies, we then  
213 applied ExpiCHO as the expression system of S-2P antigen for clinical studies and stable clones for commercial  
214 production. The S-2P proteins produced in CHO cells and their structure displayed typical spike trimers under  
215 cryo-EM (Figure S3), resembling that of Expi293-expressed SARS-CoV-2 S protein, suggesting that CHO cells  
216 are feasible in production of S-2P. The above immunogenicity studies showed that the oil in water adjuvant

217 (Sigma adjuvant) vaccinated S-2P could induce effective neutralizing antibody in mice. However, since Sigma  
218 adjuvant is not permitted for human therapeutic use and the potential of alum salts in producing Th2-mediated  
219 immunopathology, we next examined the potential of Th1-biasing CpG 1018 for clinical use. Aluminum  
220 hydroxide was also explored in the following experiment instead of aluminum phosphate as it has been  
221 characterized to enhance the potency of CpG adjuvant when used in combination while also retaining the  
222 property of inducing Th1 responses [17]. The pseudovirus neutralization assay was performed with sera drawn  
223 two weeks after the second injection. At 1  $\mu$ g of S-2P, the reciprocal ID<sub>50</sub> GMT of S-2P adjuvanted with CpG  
224 1018, aluminum hydroxide, and with both CpG 1018 and aluminum hydroxide were 245, 3,109, and 5,120,  
225 respectively (Figure 1). Similar values were obtained at 5  $\mu$ g of S-2P (Figure 1). Weaker neutralization titers  
226 were observed at 3 weeks after the first injection (Figure S4). Sera from these mice were then examined for the  
227 amount of anti-S IgG. CpG 1018 in combination with aluminum hydroxide produced significantly higher titers  
228 of anti-S IgG compared to CpG 1018 or aluminum hydroxide alone (Figure 2). The immune sera were further  
229 tested for their neutralization capabilities against wild-type SARS-CoV-2 in a neutralization assay. S-2P was  
230 able to inhibit SARS-CoV-2 at a concentration of 1  $\mu$ g, although at lower potency than that of pseudovirus  
231 (Figures 1 and 3). The reciprocal ID<sub>50</sub> GMT of S-2P in the presence of CpG 1018, aluminum hydroxide, and  
232 with both CpG 1018 and aluminum hydroxide were approximately 60, 250, and 1,500, respectively (Figure 3).  
233 Pseudovirus carrying the current dominant D614G variant spike was also generated and neutralizing antibodies  
234 from mice immunized with S-2P with CpG 1018 and aluminum hydroxide were effective against both  
235 pseudoviruses carrying the wild-type D614 and mutant D614G versions of spike proteins (Figure 4).  
236 Neutralization titers of wild-type virus and pseudovirus and total anti-S IgG titers were all found to be highly  
237 correlated with Spearman's rank correlation coefficients greater than 0.8 (Figure 5).

238

### 239 **CpG 1018 induced Th1 immunity**

240 To identify whether CpG 1018 could induce Th1 responses in our vaccine-adjuvant system, cytokines  
241 involved in Th1 and Th2 responses were measured in splenocytes from mice immunized with S-2P with  
242 aluminum hydroxide, CpG 1018, or combination of the two. As expected, S-2P adjuvanted with aluminum

243 hydroxide induced limited amounts of IFN- $\gamma$  and IL-2, the representative cytokines of Th1 response. In contrast,  
244 significant increases in IFN- $\gamma$  and IL-2 were detected most strongly in high antigen dose plus CpG 1018 and  
245 aluminum hydroxide (Figure 6). For Th2 response, while the levels of IL-4, IL-5 and IL-6 increased in the  
246 presence of aluminum hydroxide and S-2P, addition of CpG 1018 to aluminum hydroxide suppressed the levels  
247 of these cytokines (Figure 7). IFN- $\gamma$  /IL-4, IFN- $\gamma$ /IL-5, and IFN- $\gamma$ /IL-6 ratios are strongly indicative of a Th1-  
248 biased response and were increased by approximately 36-, 130-, and 2-fold, respectively, in the presence of S-  
249 2P combined with CpG 1018 and aluminum hydroxide (Figure 8). These results suggested that the effect of  
250 CpG 1018 is dominant over aluminum hydroxide in directing the cell-mediated response towards Th1 response,  
251 while retaining high antibody levels.

252

253 **S-2P did not result in systemic adverse effects in rats**

254 To elucidate the safety and potential toxicity of the vaccine candidate, 5  $\mu$ g, 25  $\mu$ g or 50  $\mu$ g of S-2P  
255 adjuvanted with CpG 1018 or CpG 1018 combined aluminum hydroxide were administered to SD rats for  
256 single-dose and repeat-dose studies. No mortality, abnormality of clinical signs, differences in body weight  
257 changes, body temperature, nor food consumption were observed in either gender that could be attributed to S-  
258 2P (with or without adjuvant) with single dose administration (Figures 9 and 10). Increased body temperature  
259 at 4-hr or 24-hr after dosing was found in both genders of single-dose study and repeat-dose study; however,  
260 these temperature changes were moderate and were recovered after 48-hr in both genders of all treated groups  
261 including controls (PBS) (Figure 9). No gross lesions were observed in organs of most of the male and female  
262 rats with single-dose and two-dose administration, except for one male rat which was deemed to be non-vaccine-  
263 related. In conclusion, S-2P protein, with CpG 1018 or CpG 1018 + aluminum hydroxide as adjuvants  
264 administrated intramuscularly once or twice to SD rats did not induce any systemic adverse effect.

265

266 **Discussion**

267

268 In this study, we showed that in mice, two injections of a subunit vaccine consisting of the prefusion spike  
269 protein (S-2P) adjuvanted with CpG 1018 and aluminum hydroxide was effective in inducing potent  
270 neutralization activity against both pseudovirus expressing wild-type and D614G variant spike proteins, and  
271 wild-type SARS-CoV-2. The combination of S-2P with CpG 1018 and aluminum hydroxide elicited Th1-  
272 dominant immune responses with high neutralizing antibody levels in mice and showed no major adverse effects  
273 in rats. We also successfully scaled-up yield of S-2P by establishing stable CHO cell clones expressing S-2P  
274 protein and improved the purification process at a sufficient quantity of antigen for the production of a  
275 commercial vaccine. Spike is a highly glycosylated protein and we chose CHO-cell production to achieve  
276 mammalian glycosylation patterns that will include complex glycans and may be important for immunogenicity.  
277 Although the leading subunit protein COVID-19 vaccines by developers such as Sanofi Pasteur and Novavax  
278 are made in baculovirus, the insect cell produce protein with man-9 glycosylation that may be sufficient for  
279 immune response induction, but may not recapitulate the antigenicity of virus grown in mammalian cells [5, 18-  
280 19]. Animal challenge studies will be conducted at a future date to examine the safety and efficacy of our  
281 candidate vaccine. Based on our results and in accordance with the International Coalition of Medicines  
282 Regulatory Authorities (ICMRA), we plan to move forward with first-in-human clinical trials and conduct  
283 preclinical studies in parallel to expedite vaccine development in the current COVID-19 pandemic.

284

285 We have successfully shown robust immunogenicity elicited by adjuvanted SARS-CoV-2 S-2 (Figures 1,  
286 2, S1, and S2). Much stronger neutralizing antibody responses were detected in mice when 1  $\mu$ g or 5  $\mu$ g of S-  
287 2P protein was adjuvanted with 10  $\mu$ g of CpG 1018 and 50  $\mu$ g of aluminum hydroxide than with either adjuvant  
288 alone (Figure 1). S-2P in conjunction with CpG 1018 and aluminum hydroxide induced potent anti-S antibodies  
289 that were effective against wild-type virus (Figures 2 and 3). We have shown that high degrees of correlation  
290 between neutralization titers of pseudovirus, wild-type virus, and anti-S IgG titers (Figure 5), raising the

291 potential that anti-S IgG titer could be used as surrogate for vaccine potency instead of performing pseudovirus  
292 or wild-type virus assays. During the course of vaccine development against fast-evolving RNA viruses such as  
293 SARS-CoV-2, it is important that the protection offered by the vaccine could extend to variants that could  
294 otherwise drastically reduce the effectiveness of neutralizing antibody. Strains harboring the D614G mutation  
295 in the spike protein were first observed in Europe in February 2020 and overtime has become the global  
296 dominant variant [20]. Our results of the pseudovirus neutralization assay showed cross-reaction of these  
297 antibodies with the dominant circulating strain D614G with similar titer levels (Figure 4). Therefore, we  
298 confirmed that S-2P was able to generate antibodies effective against both the original wild-type strain and its  
299 variant. Neutralization titers of antibodies against different strains of wild-type viruses should be investigated  
300 in the future, but our results indicate the potential of this candidate vaccine to provide broad spectrum protection  
301 against COVID-19 infection.

302

303       Although moderate IL-4 production was detected in mice receiving 5 µg of S-2P combined with CpG 1018  
304 and aluminum hydroxide, the IFN- $\gamma$ /IL-4 ratio was 16-fold higher than those receiving 5 µg of S-2P adjuvanted  
305 with aluminum hydroxide alone. These results suggested that CpG 1018, even in the presence of aluminum  
306 hydroxide could steer the immune response away from Th2 to a Th1 response. Moreover, these mice produce a  
307 limited amount of IL-5, which is a key mediator in eosinophil activation and major regulator of eosinophil  
308 accumulation in tissues [21]. Previous studies showed that the lung-infiltrating eosinophils were a common  
309 indication of Th2-biased immune responses seen in animal models testing SARS-CoV vaccine candidates [22].  
310 The finding that IL-5 production was inhibited by the S-2P adjuvanted with CpG 1018 plus aluminum hydroxide  
311 suggests that it would be less likely to induce immune responses resulting in eosinophil infiltration in lung. Th1  
312 and Th2-biased responses are determined by factors, including administration routes, antigen and adjuvant  
313 characteristics, and cytokines [11]. Our results showed that S-2P per se is unlikely to skew the immune response  
314 towards Th1, but in the presence of an adjuvant such as CpG 1018, S-2P can direct the immune response towards  
315 Th1. Thus, we have shown that S-2P adjuvanted with CpG 1018 plus aluminum hydroxide is a potential  
316 formulation for COVID-19 vaccine development.

317 Single-dose or repeat-dose administration of S-2P protein adjuvanted with CpG 1018 and aluminum  
318 hydroxide was well tolerated in rats in both genders, supporting human clinical trials in young healthy adults.  
319 GLP toxicology study of S-2P in combination of higher dose of CpG 1018 and aluminum hydroxide will be  
320 conducted to explore safety of the formulated S-2P for dose escalation study in human clinical trials with the  
321 elderly and those with chronic health conditions such as diabetes and cardiovascular diseases, who may require  
322 a higher adjuvant dose to boost the immune systems. As a two-dose regimen of S-2P formulated with CpG 1018  
323 and aluminum hydroxide induced potent neutralizing activity, our future plans will include testing single-dose  
324 regimens.

325 Our study showed that CHO-derived S-2P proteins elicited robust immune responses in mice, indicating  
326 that CHO cell is an appropriate platform for stable S-2P production in vaccine development. Other vaccines  
327 using CHO cells to produce antigens include hepatitis B vaccines GenHevacB and Sci-B-Vac [23]. To this date,  
328 we have established stable CHO cell clones expressing S-2P and the one with the highest yield will be selected  
329 to produce master cell bank for large scale GMP production of commercial vaccine.

330

331 The rapid spread of SARS-CoV-2 and urgent need for an effective vaccine call for its development using  
332 readily available and proven technologies. The spike protein is the main receptor binding and membrane fusion  
333 protein, which serves as the major antigen target for COVID-19 vaccine development. We have demonstrated  
334 in this study that the S-2P combined with the advanced adjuvant CpG 1018, the adjuvant contained in the FDA-  
335 approved adult hepatitis B vaccine (HEPLISAV-B), in combination with aluminum hydroxide induced potent  
336 Th1-biased immune responses to prevent wild-type virus infections while retaining high antibody levels that  
337 show cross-neutralization of variant viruses. Therefore, this vaccine formulation serves as an ideal vaccine  
338 candidate in alleviating the burden of the global COVID-19 pandemic.

339

340

341

342 **Acknowledgements**

343

344 We thank Dr. Barney S. Graham, Dr. Kizzmekia S. Corbett and members of the Graham lab for providing the  
345 S-2P plasmid and initial batch of S-2P protein, as well as providing technical guidance and helpful advices. We  
346 are grateful for the participation of Dr. Michael D. Malison, Dr. Han van den Bosch, Dr. Ya-Shan Chuang, and  
347 Yu-Fan Tu for manuscript preparation and constructive comments. In addition, we would like to acknowledge  
348 Dr. Yu-Chi Chou for the pseudovirus neutralization assay at the RNAi Core Facility, Academia Sinica. We also  
349 thank team members at TFBS Bioscience Incorporation for animal experiments and cytokine detection.

350

351 **References**

352

- 353 1. Zhou P, Yang XL, Wang XG, Hu B, Zhang L, Zhang W, Si HR, Zhu Y, Li B, Huang CL, Chen HD. Discovery  
354 of a novel coronavirus associated with the recent pneumonia outbreak in humans and its potential bat origin.  
355 BioRxiv. 2020 Jan 1.
- 356 2. ArcGIS Dashboards. Gisanddata.maps.arcgis.com. 2020 [retrieved 05 August 2020]. Available from:  
357 <https://gisanddata.maps.arcgis.com/apps/opsdashboard/index.html#/bda7594740fd40299423467b48e9ecf6>
- 358 3. Gates B. Responding to Covid-19—a once-in-a-century pandemic?. New England Journal of Medicine. 2020  
359 Apr 30;382(18):1677-9.
- 360 4. Schäferhoff M, Yamey G, McDade K. Funding the development and manufacturing of COVID-19 vaccines: The  
361 need for global collective action. Brookings. 2020 [retrieved 1 June 2020]. Available from:  
362 <https://www.brookings.edu/blog/future-development/2020/04/24/funding-the-development-and-manufacturing-of-covid-19-vaccines-the-need-for-global-collective-action/>
- 364 5. WHO R&D Blueprint. DRAFT Landscape of COVID-19 Candidate Vaccines – 31 July 2020. Available from:  
365 <https://www.who.int/who-documents-detail/draft-landscape-of-covid-19-candidate-vaccines>
- 366 6. WHO R&D Blueprint. Target Product Profiles for COVID-19 Vaccines – 17 April 2020. Available from:  
367 <https://www.who.int/who-documents-detail/who-working-group-target-product-profiles-for-covid-19-vaccines>
- 368 7. Gorbatenko AE. Severe acute respiratory syndrome-related coronavirus—The species and its viruses, a statement  
369 of the Coronavirus Study Group. BioRxiv. 2020 Jan 1.
- 370 8. Pallesen J, Wang N, Corbett KS, Wrapp D, Kirchdoerfer RN, Turner HL, Cottrell CA, Becker MM, Wang L,  
371 Shi W, Kong WP. Immunogenicity and structures of a rationally designed prefusion MERS-CoV spike antigen.  
372 Proceedings of the National Academy of Sciences. 2017 Aug 29;114(35):E7348-57.
- 373 9. Wrapp D, Wang N, Corbett KS, Goldsmith JA, Hsieh CL, Abiona O, Graham BS, McLellan JS. Cryo-EM  
374 structure of the 2019-nCoV spike in the prefusion conformation. Science. 2020 Mar 13;367(6483):1260-3.
- 375 10. Lee S, Nguyen MT. Recent advances of vaccine adjuvants for infectious diseases. Immune network. 2015 Apr

376 1;15(2):51-7.

377 11. Shi S, Zhu H, Xia X, Liang Z, Ma X, Sun B. Vaccine adjuvants: Understanding the structure and mechanism of  
378 adjuvanticity. *Vaccine*. 2019 May 27;37(24):3167-78.

379 12. Tseng CT, Sbrana E, Iwata-Yoshikawa N, Newman PC, Garron T, Atmar RL, Peters CJ, Couch RB.  
380 Immunization with SARS coronavirus vaccines leads to pulmonary immunopathology on challenge with the  
381 SARS virus. *PLoS one*. 2012 Apr 20;7(4):e35421.

382 13. Hotez PJ, Corry DB, Bottazzi ME. COVID-19 vaccine design: the Janus face of immune enhancement. *Nature  
383 Reviews Immunology*. 2020 Jun;20(6):347-8.

384 14. Campbell JD. Development of the CpG adjuvant 1018: a case study. In *Vaccine Adjuvants 2017* (pp. 15-27).  
385 Humana Press, New York, NY.

386 15. Huang CG, Lee KM, Hsiao MJ, Yang SL, Huang PN, Gong YN, Hsieh TH, Huang PW, Lin YJ, Liu YC, Tsao  
387 KC. Culture-based virus isolation to evaluate potential infectivity of clinical specimens tested for COVID-19.  
388 *Journal of Clinical Microbiology*. 2020 Jun 9.

389 16. Lu B, Huang Y, Huang L, Li B, Zheng Z, Chen Z, Chen J, Hu Q, Wang H. Effect of mucosal and systemic  
390 immunization with virus-like particles of severe acute respiratory syndrome coronavirus in mice. *Immunology*.  
391 2010 Jun;130(2):254-61.

392 17. Thomas LJ, Hammond RA, Forsberg EM, Geoghegan-Barek KM, Karalius BH, Marsh, Jr HC, Rittershaus CW.  
393 Co-administration of a CpG adjuvant (VaxImmuneTM, CPG 7909) with CETP vaccines increased  
394 immunogenicity in rabbits and mice. *Human vaccines*. 2009 Feb 1;5(2):79-84.

395 18. Tian JH, Patel N, Haupt R, Zhou H, Weston S, Hammond H, Lague J, Portnoff AD, Norton J, Guebre-Xabier M,  
396 Zhou B. SARS-CoV-2 spike glycoprotein vaccine candidate NVX-CoV2373 elicits immunogenicity in baboons  
397 and protection in mice. *bioRxiv*. 2020 Jan 1.

398 19. O'Flaherty R, Bergin A, Flampouri E, Mota LM, Obaidi I, Quigley A, Xie Y, Butler M. Mammalian cell culture  
399 for production of recombinant proteins: A review of the critical steps in their biomanufacturing. *Biotechnology  
400 Advances*. 2020 May 13:107552.

401 20. Korber B, Fischer WM, Gnanakaran S, Yoon H, Theiler J, Abfalterer W, Hengartner N, Giorgi EE, Bhattacharya  
402 T, Foley B, Hastie KM. Tracking changes in SARS-CoV-2 Spike: evidence that D614G increases infectivity of  
403 the COVID-19 virus. *Cell*. 2020 Jul 3.

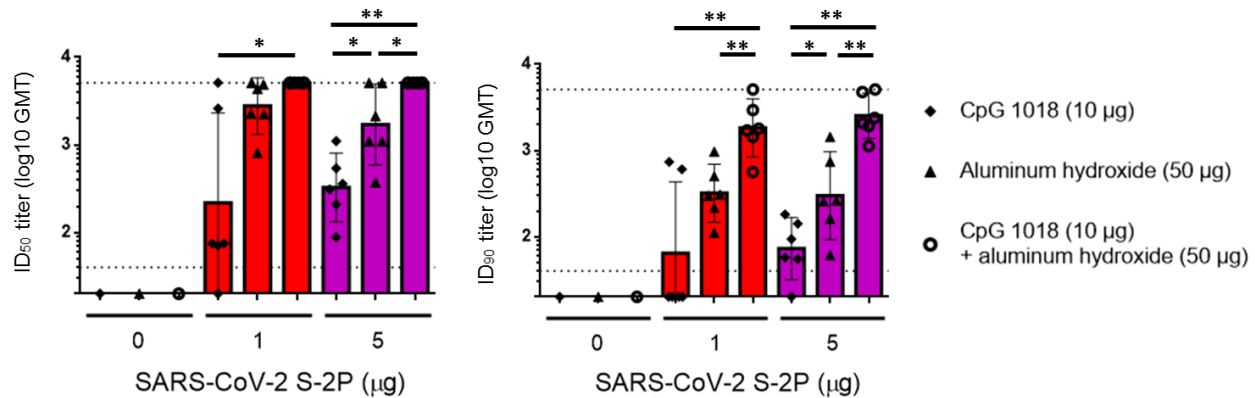
404 21. Lopez AF, Begley CG, Williamson DJ, Warren DJ, Vadas MA, Sanderson CJ (May 1986). "Murine eosinophil  
405 differentiation factor. An eosinophil-specific colony-stimulating factor with activity for human cells". *J. Exp.  
406 Med.* 163 (5): 1085–1099.

407 22. Tseng CT, Sbrana E, Iwata-Yoshikawa N, et al. Immunization with SARS coronavirus vaccines leads to  
408 pulmonary immunopathology on challenge with the SARS virus [published correction appears in *PLoS One*.  
409 2012;7(8). doi:10.1371/annotation/2965cfae-b77d-4014-8b7b-236e01a35492]. *PLoS One*. 2012;7(4):e35421.  
410 doi:10.1371/journal.pone.0035421

411 23. Perazzo P, Valle NRD, Sordelli A, Gonzalez RH, Cuestas ML, et al. (2015) Nanotechnology, Drug Delivery  
412 Systems and their Potential Applications in Hepatitis B Vaccines. *Int J Vaccines Vaccin* 1(2): 00007.

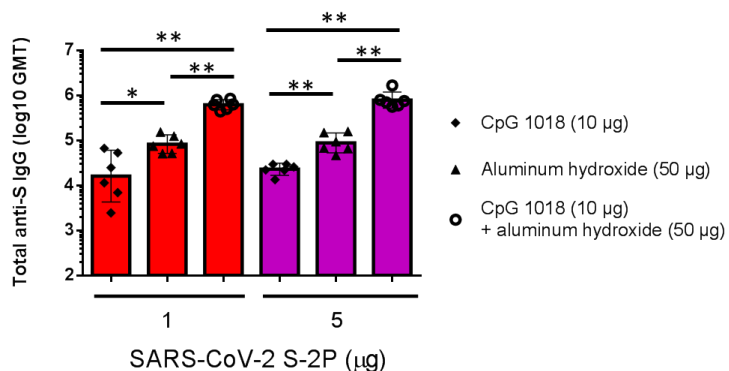
413

414 **Figures**



415

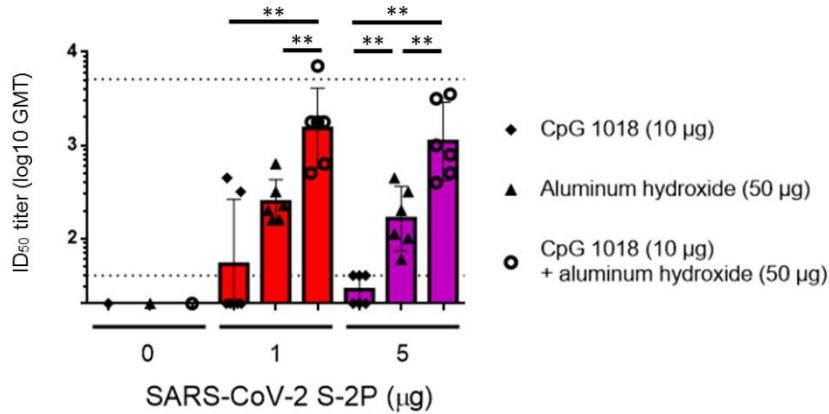
416 **Figure 1. Induction of neutralizing antibodies by CpG 1018 and aluminum hydroxide-adjuvanted SARS-**  
417 **CoV-2 S-2P 2 weeks post-second injection.** BALB/c mice were immunized with 2 dose levels of CHO cell-  
418 expressed SARS-CoV-2 S-2P adjuvanted with CpG 1018, aluminum hydroxide or combination of both 3 weeks apart  
419 and the antisera were harvested at 2 weeks after the second injection. The antisera were subjected to neutralization  
420 assay with pseudovirus expressing SARS-CoV-2 spike protein to determine the  $ID_{50}$  (left) and  $ID_{90}$  (right) titers of  
421 neutralization antibodies.



422

423 **Figure 2. Total anti-S IgG titers in mice immunized with S-2P with adjuvants.** Sera from BALB/c mice in  
424 Figure 1 immunized with 1 or 5  $\mu$ g of S-2P with CpG 1018, aluminum hydroxide or combination of both were  
425 quantified for the total amount of anti-S IgG with ELISA.

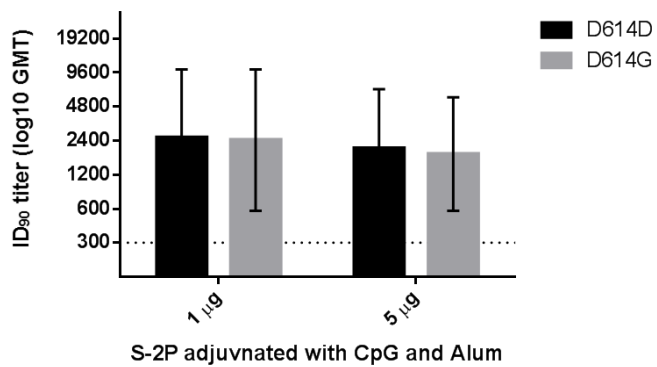
426



427

428 **Figure 3. Neutralization of wild-type SARS-CoV-2 virus by antibodies induced by SARS-CoV-2 S-2P**  
429 **adjuvanted with CpG 1018 and aluminum hydroxide.** The antisera were collected as described in Figure 2 and  
430 subjected to a neutralization assay with wild-type SARS-CoV-2 to determine neutralization antibody titers.

431

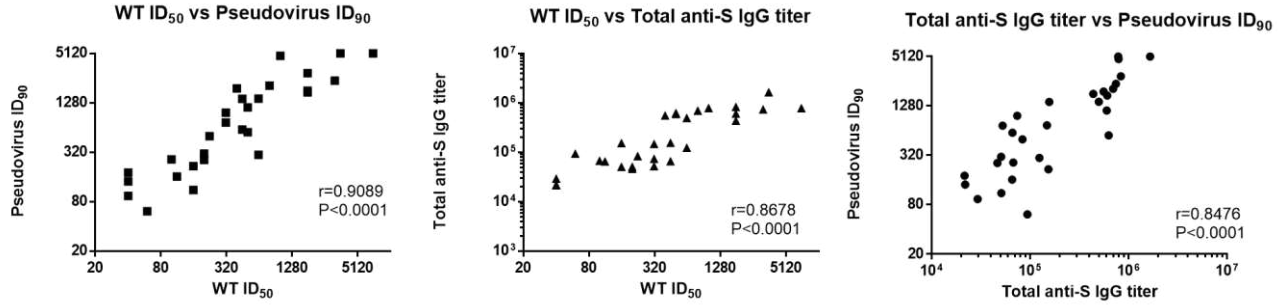


432

433 **Figure 4. Inhibition of pseudoviruses carrying D614D (wild-type) or D614G (variant) versions of the spike**  
434 **protein by mice immunized with S-2P with CpG 1018 and aluminum hydroxide.** The antisera of BALB/c mice  
435 immunized with 1 or 5 μg of S-2P with 10 μg CpG 1018 and 50 μg aluminum hydroxide as in Figure 1 were collected.  
436 Neutralization assays were performed with pseudoviruses with either D614D or D614G spike proteins.

437

438

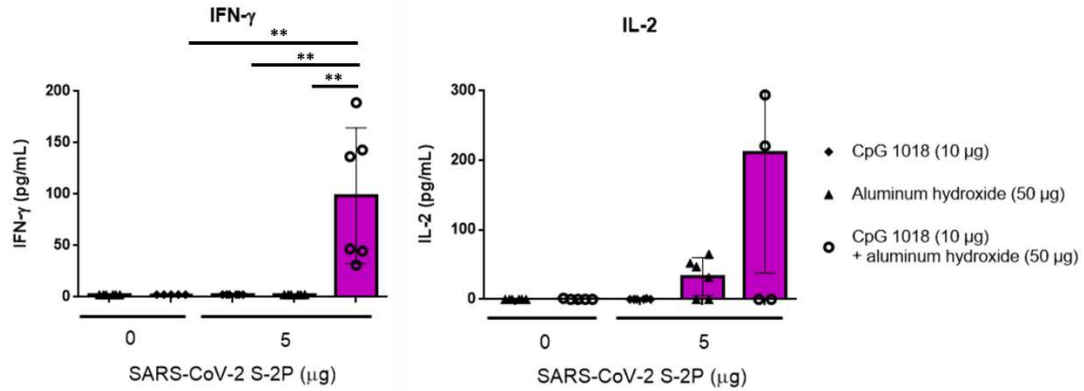


439

440

441 **Figure 5. Correlations between SARS-CoV-2 pseudovirus ID<sub>90</sub>, wild-type SARS-CoV-2 ID<sub>50</sub>, and total**  
442 **anti-S IgG titers in mice.** Values were tabulated and correlations were calculated with Spearman's rank correlation  
443 coefficient for wild-type SARS-CoV-2 ID<sub>50</sub> vs pseudovirus ID<sub>90</sub> (left), wild-type SARS-CoV-2 ID<sub>50</sub> vs total anti-S  
444 IgG titer (middle), and pseudovirus ID<sub>90</sub> vs total anti-S IgG titer (right).

445

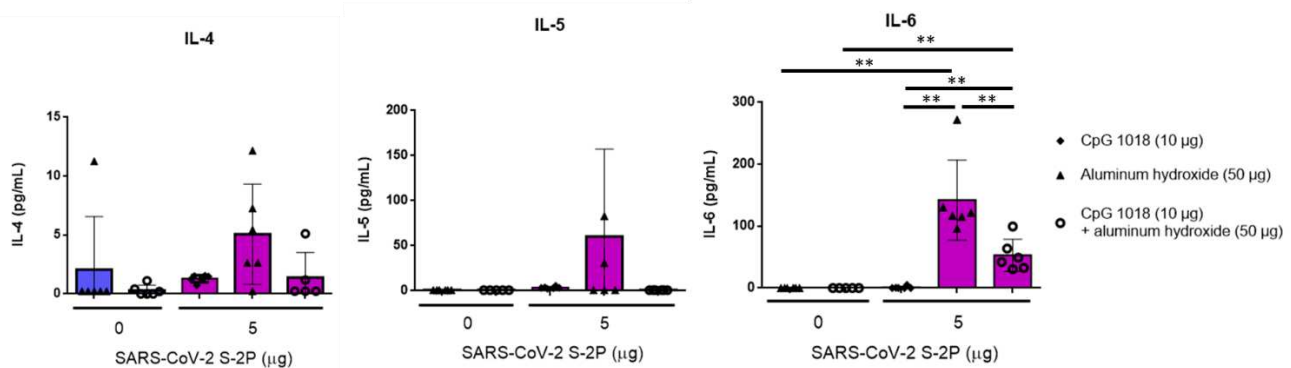


446

447 **Figure 6. Th1-dependent cytokine production induced by SARS-CoV-2 S-2P adjuvanted with CpG 1018,**  
448 **Aluminum hydroxide, or CpG 1018/Aluminum hydroxide in mice.** Two weeks after the second injection, the  
449 splenocytes were harvested and incubated with S-2P protein (5 μg), Concanavalin A (0.1 μg; data not shown) for  
450 positive control, or complete RPMI 1640 medium only for negative control. After 20 hours incubation, the levels of  
451 IFN-γ (left) and IL-2 (right) were analyzed by ELISA.

452

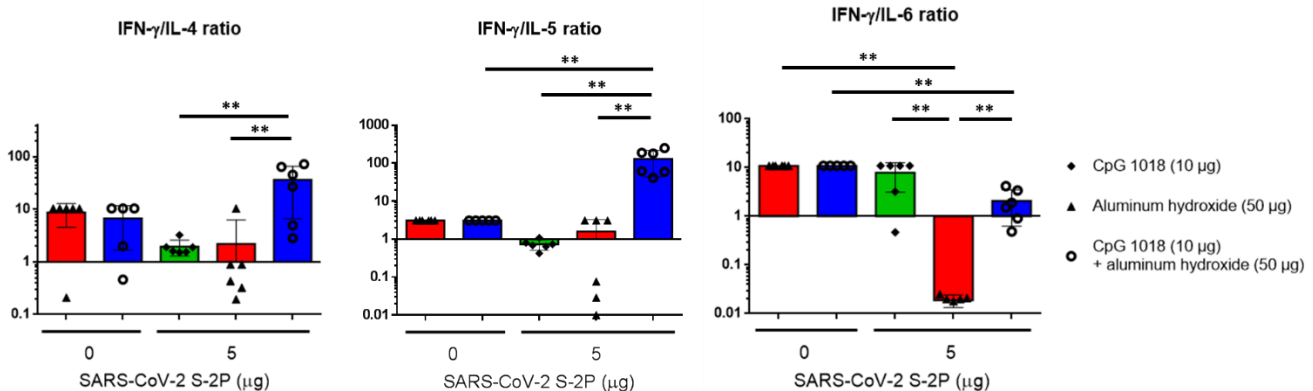
453



454

455 **Figure 7. Th2-dependent cytokine production induced by SARS-CoV-2 S-2P adjuvanted with CpG 1018,**  
456 **Aluminum hydroxide, or CpG 1018/Aluminum hydroxide in mice.** Two weeks after the second injection, the  
457 splenocytes were harvested and stimulated as in Fig. 6. After 20 hours incubation, the levels of IL-4 (left), IL-5  
458 (middle), and IL-6 (right) released from the splenocytes were analyzed. For detection of cytokines, the culture  
459 supernatant was harvested to analyze the levels of cytokines by ELISA.

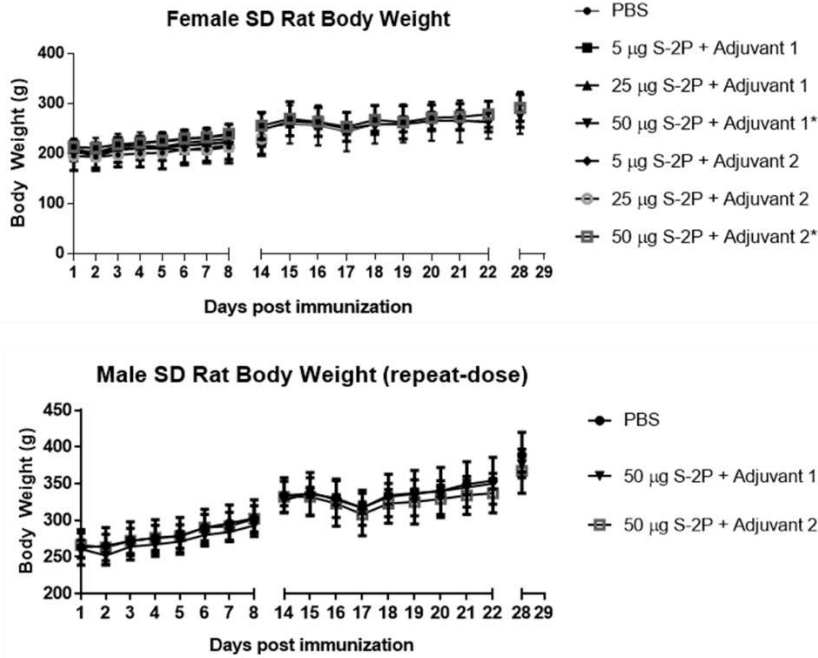
460



461

462 **Figure 8. IFN- $\gamma$  /IL-4, IFN- $\gamma$ /IL-5, and IFN- $\gamma$ /IL-6 ratios.** IFN- $\gamma$ , IL-4, IL-5, and IL-6 values from the  
463 cytokine assays were used to calculate ratios. Ratio values greater than 1 indicate Th-1 bias whereas ratio less than 1  
464 indicate Th-2 bias responses.

465



466

467 **Figure 9. Female (top) and male (bottom) body weight of SD rats immunized with indicated amount of S-  
468 2P with adjuvants. Adjuvant 1 = CpG 1018, Adjuvant 2 = CpG 1018 + aluminum hydroxide.**

469

470

471

472

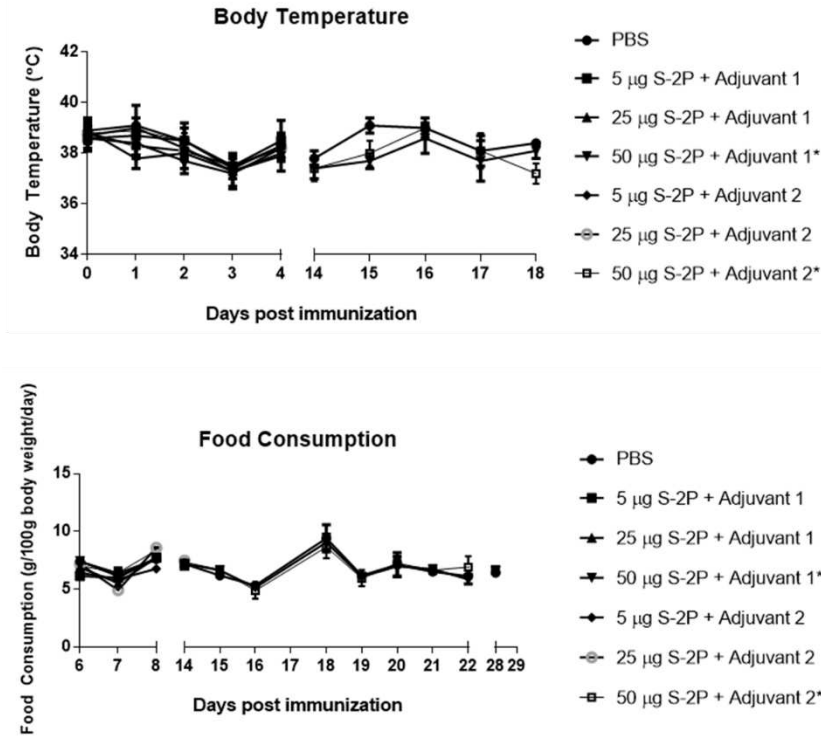
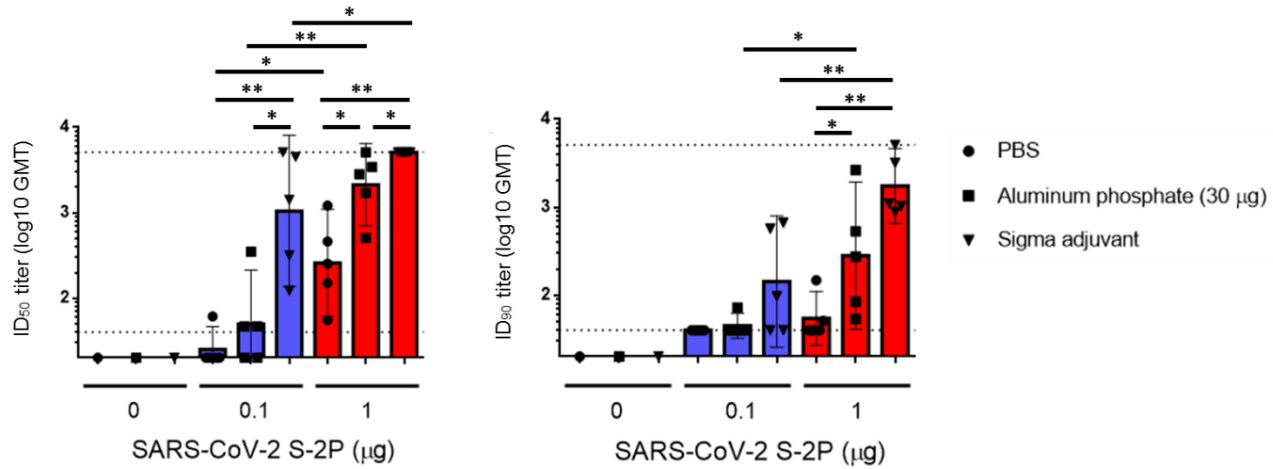


**Figure 10. Body temperature (top) and food consumption (bottom) of female and male SD rats**

immunized with indicated amount of S-2P with adjuvants. Adjuvant 1 = CpG 1018, Adjuvant 2 = CpG 1018 + aluminum hydroxide.

477



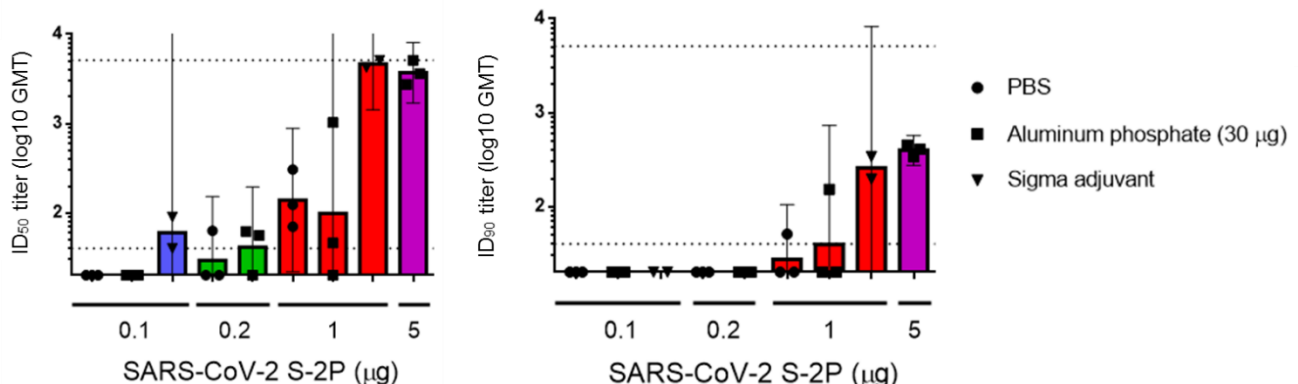
478

479 **Figure S1. Immunogenicity elicited by adjuvanted SARS-CoV-2 S-2P.** BALB/c mice were immunized with  
480 2 injections of HEK 293 cell-expressed SARS-CoV-2 S-2P alone or combined with various adjuvants 3 weeks apart  
481 and the antisera were harvested at 2 weeks after the second injection. The antisera were subjected to a neutralization  
482 assay with pseudovirus expressing SARS-CoV-2 spike protein to determine the  $ID_{50}$  (left) and  $ID_{90}$  (right) titers of  
483 neutralization antibodies.

484

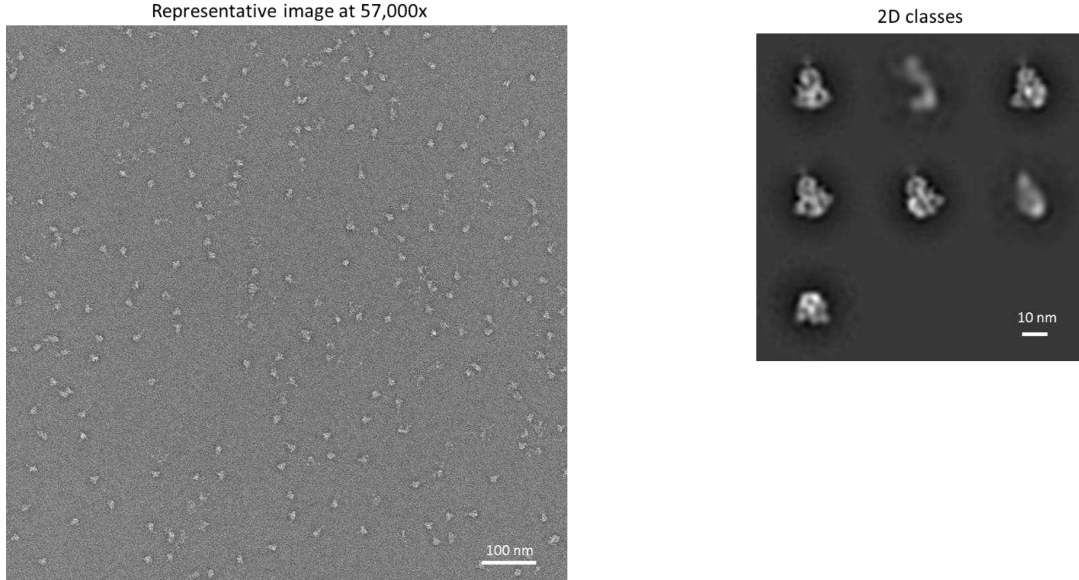
485

486



487

488 **Figure S2. Neutralization antibodies induced by adjuvanted SARS-CoV-2 S-2P.** BALB/c mice were  
489 immunized with different dose levels of Expi293 cell-expressed SARS-CoV-2 S-2P protein as described in Figure 1.  
490 2 weeks after the second injection, the antisera were subjected to neutralization assay with pseudovirus expressing  
491 SARS-CoV-2 spike protein to determine the  $ID_{50}$  (left) and  $ID_{90}$  (right) titers of neutralization antibodies.



493

**Figure S3. Assembled spike trimers of SARS-CoV2 S-2P under EM (left) and corresponding to ordered**

494

**spike molecules 2D classes (right).** SARS-CoV2 S-2P was transiently expressed by ExpiCHO cells. The sample

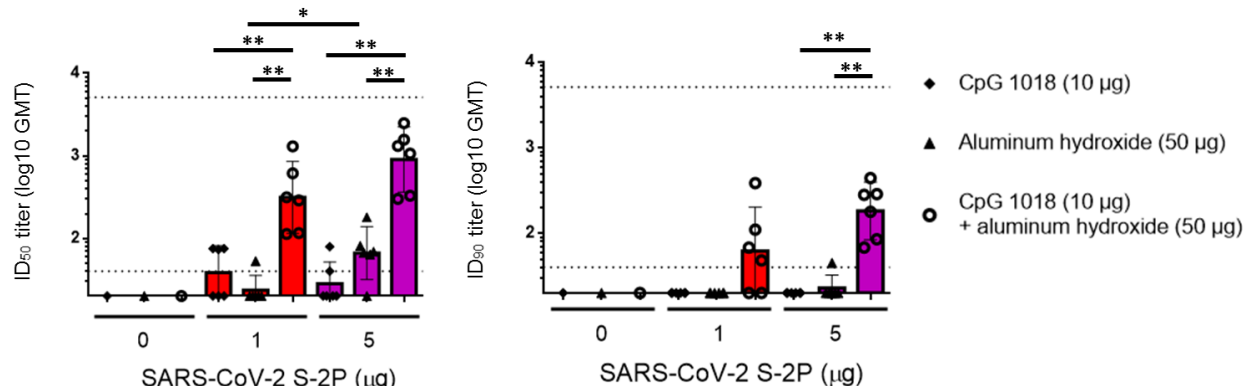
495

contains primarily assembled spike trimers. Most particles contributed to 2D classes corresponding to ordered spike

496

molecules.

497



498

**Figure S4 Neutralizing antibody responses in BALB/c mice 3 weeks after first injection of CpG 1018 and**

499

**aluminum hydroxide-adjuvanted SARS-CoV-2 S-2P.** BALB/c mice were immunized with 2 injections of CHO

500

cell-expressed SARS-CoV-2 S-2P adjuvanted with CpG 1018, aluminum hydroxide or combination of both 3 weeks

501

apart and the antisera were harvested at 3 weeks after the first injection. The antisera were subjected to neutralization

502

assay with pseudovirus expressing SARS-CoV-2 spike protein to determine the ID<sub>50</sub> (left) and ID<sub>90</sub> (right) titers of

503

neutralization antibodies.

504